APPLICATION OF HIGH RESOLUTION MASS SPECTROMETRY

IN MOLECULAR STRUCTURE STUDIES

A. L. Burlingame

Department of Chemistry and Space Sciences Laboratory
University of California, Berkeley, California, 94720

NASA CR.56913

Abstract:

Automatic Data Reduction from high-resolution mass spectrograms is described. Elucidation of fragmentation mechanisims of Amaryllidaceae and Lycopodium alkaloids via accurate mass measurement of all major fragments in the high resolution mass spectrogram is discussed.

Introduction:

A decade ago the potentialities of double-focusing mass spectrometry were recognized by Beynon [1] who demonstrated that accurate mass measurement of an ion could render unique characterization of its empirical composition. In this early work, use was made of the Nier-Johnson geometry embodied in the MS-8 mass spectrometer [1] - a predecessor of A. E. I. 's current MS-9.

In this laboratory, the Mattauch-Herzog geometry is employed in the C. E. C. 21-110 mass spectrometer/spectrograph. Studies in progress in our laboratory center around two basic problems: (a) the capability of accurate mass measurement of many ions in a single mass spectrum; and the related problem (b) the capability of obtaining as much mass spectral data as possible on extremely small amounts of sample. Therefore, the simultaneous, permanent registration of an entire mass spectrum on a photoplate at highest attainable resolution consistant with unique characterization of empirical composition is of utmost importance in our studies. The combination photoplate, ion multiplier employed in the Mattauch-Herzog

REPORTS CONTROL No._____

  - 2 -

configuration allows such versatility. Many of the advantages and disadvantages of such an approach have been noted by Biemann [2].

I. Experimental Techniques:

A direct sample inlet system for introduction of (a) solids of low volatility and (b) thermally labile compounds has been constructed in our laboratory as shown in Figure 1.

The system is all glass with the exception of the teflon probe, and heated as one unit. The vacuum lock valve will hold 10^{-7} mm Hg in the ion source when exposed to atmospheric pressure. This direct inlet has a ground glass ball joint valve and its own vacuum system. This has the advantage of our being able to pump samples out directly from the direct inlet line without necessitating the complete pump out through the source chamber.

II. Automatic Data Reduction from Photoplate.

The chief experimental problem involved in high resolution mass spectrography is the reduction of data from the photoplate. In our laboratory, a digitized, high-precision automatic recording microphotometer is employed to give simultaneously line position (in microns) and plate blackening (in percent transmission). These data are read out on an IBM card punch during the microphotometer tracing of the high resolution spectrogram. The precision of linear measurement is ± 1 micron which corresponds to about one millimass unit at normal dispersion on the photoplate up to mass 400. Data for the average deviation of our measurements is indicated in the various tables of data. The accurate mass in calculated via a quadratic interpolation using fluorocarbon mass calibration. All accurate mass measurements reported in this paper were carried out automatically.

The Jarrall-Ash (Model 23-500) Recording High-Precision Microphotometer was employed with Wang Laboratories digitizing apparatus in this study.

III. Elucidation of Fragmentation Mechanisms via Determination of the

Empirical Composition of Major Ions in a High Resolution Mass

Spectrogram.

A. Representatives of the crinine series in the family of Amaryllidaceae
alkaloids[*].

Recent application of high resolution mass spectrometry to natural

products chemistry has resulted in the clarification of the electron-impact-

induced fragmentation of ajmalidine and related substances [3] and the de-

termination of the empirical composition of the dimeric alkaloid, vinblastine,

by accurate mass measurement of its molecular ion peak [4].

In connection with the determination of the structure of Amaryllisine

(1), an Amaryllidaceae alkaloid possessing the 5,10b-ethano-3,4,4a,5,6,10b-

hexahydrophenanthridine carbon skeleton, the mass spectra of several alka-

loids in the crinine series were examined by low resolution mass spectrometry.

From these conventional mass spectra of buphanisine (2), Fig. 2, and

dihydrobuphanisine (3), Fig. 3, it was noted that reduction of the 1,2-double

bond altered drastically the fragmentation pattern of the basal carbon skeleton [5].

(1)   (2)   (3)

---
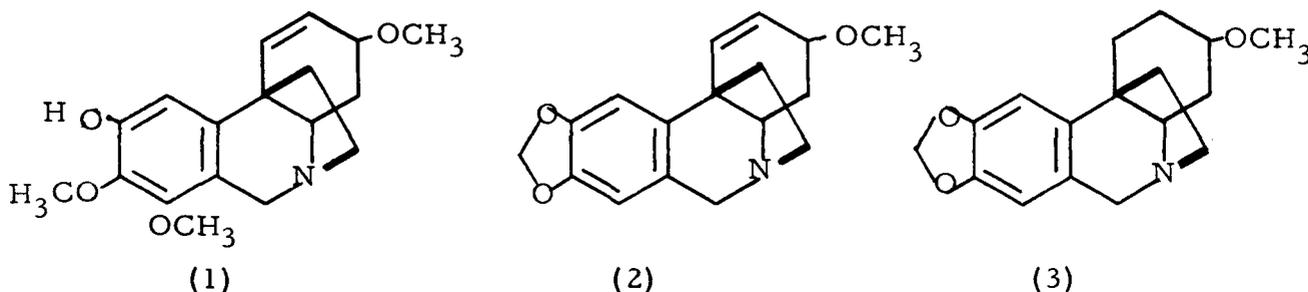
[*]Comprehensive reviews of the chemistry of these alkaloids may be found
in: W. C. Wildman in The Alkaloids, R. H. S. Manske, ed., Academic
Press, Inc., New York, 1960, Vol. VI, p. 289; and H.-G. Boit,
Ergebenisse der Alkaloid-chemie bis 1960, Academie-Verlag, Berlin,
1961, p. 410

SCHEME I

(2)   "A"

"B"

M/E 230

M/E 215
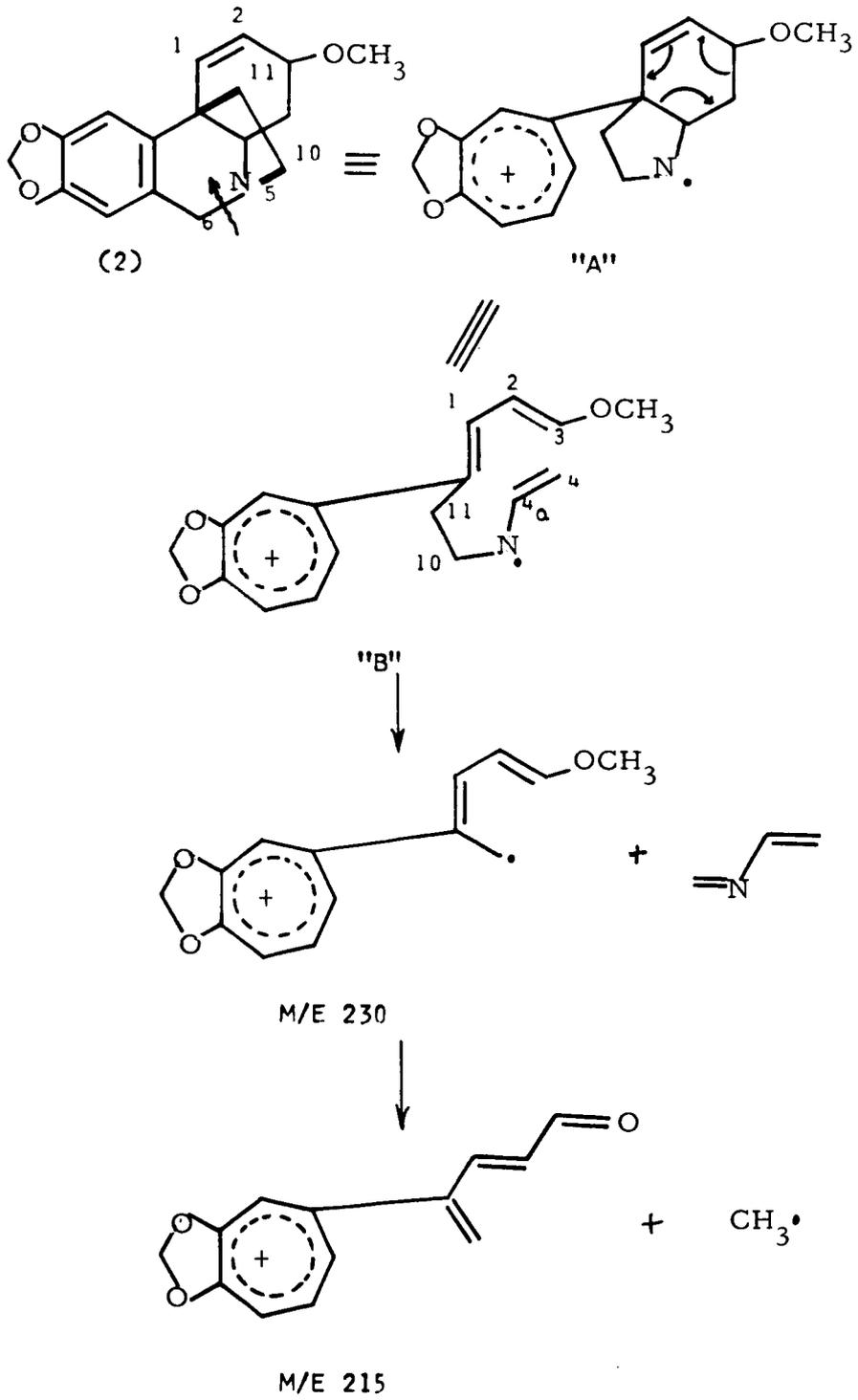
From these low resolution studies, mechanistic rationalization of the modes of fragmentation operative in these alkaloids was difficult and, at best, ambiguous.   This appeared particularly true assuming that the alicyclic nitrogen directed the major modes of cleavage in the alicyclic moiety as has been found to be the case in the indole alkaloids [6].   On this account, it seemed appropriate to determine the elemental compositions of all major ions in the high resolution mass spectra of these compounds.

Accurate mass measurements for buphanisine (2), which are listed in Table 1, revealed that the composition of fragments at M-55 and M-70 do not contain the alicyclic nitrogen.   This was indeed suprising and led to the fragmentation sequence depicted in Scheme I.   Cleavage of the 5, 6-bond in buphanisine with charge retention on the tropilium moiety forms a species "a" which can undergo a retro-Diels-Alder fission of ring C resulting in the "open" molecular ion, "b".   Simple fission of the 10, 11-bond in the "open" ion "b" forms the conjugated allylic radical-tropilium type ion (M-55) of composition $C_{14}H_{14}O_3$ via elimination of the neutral, unsaturated nitrogen moiety.

Now, facile loss of a methyl radical from the M-55 fragment results in formation of the highly unsaturated, substituted tropylium ion at m/e 215 (M-70).   A large metastable peak is observed for the 230 → 215 transition in the conventional mass spectrum.

Peaks at M-15 and M-31 correspond to loss of methyl and methoxyl radical from the molecular ion respectively.

Turning to the conventional spectrum of dihydrobuphanisine (3) shown in Figure 3, it is apparent that reduction of the 1, 2-double bond has altered the fragmentation of the carbon skeleton drastically.   This is further emphasized from analysis of the high resolution data, since the major fragments now contain nitrogen and elimination of a nitrogen

TABLE I

Accurate mass measurement of Buphanisine (2) :

measured mass	error (obs. -calc.) in m. m. u.	elemental composition
172.0510	-1.4	$C_{11}H_8O_2$
185.0588	-1.5	$C_{12}H_9O_2$
198.0658	-2.3	$C_{13}H_{10}O_2$
201.0772	-1.7	$C_{12}H_{11}NO_2$
215.0718	+1.0	$C_{13}H_{11}O_3$
230.0927	-1.6	$C_{14}H_{14}O_3$
253.1076	-2.7	$C_{16}H_{15}NO_2$
257.1046	-0.6	$C_{15}H_{15}NO_3$
270.1113	-1.8	$C_{16}H_{16}NO_3$
285.1355	-0.9	$C_{17}H_{19}NO_3$

Accurate mass measurement of Dihydrobuphanisine (3) :

174.0687	+0.6	$C_{11}H_{10}O_2$
185.0613	+1.1	$C_{12}H_9O_2$
201.0817	+2.8	$C_{12}H_{11}NO_2$
226.0906	+3.8	$C_{14}H_{12}NO_2$
256.1347	+0.9	$C_{16}H_{18}NO_2$
272.1290	+0.4	$C_{16}H_{18}NO_3$
288.1594	-0.6	$C_{17}H_{22}NO_3$ i. e. $C_{16}C^{13}H_{21}NO_3$

moiety is prevented in this saturated alicyclic derivative.

Peaks at M-61 and M-86 correspond to losses of C_3H_9O and $C_5H_{10}O$ respectively from the molecular composition. These most probably have their origin in elimination of ring C.

Thus, it can be seen that high resolution data greatly facilitates the interpretation of the fragmentation of complex molecules by providing unambiguous determination of the empirical composition of all the peaks produced on electron bombardment of a complex natural product.

B. Structure Correlations in Lycopodium alkaloids

Recently, MacLean [7] has reported the mass spectra of representative Lycopodium alkaloids of known structure and has interpreted these low resolution mass spectra in terms of the molecular structure of the compounds. Deuterium labeling was employed in some cases in an attempt to clarify the fragmentation mechanisms proposed for the basal carbon skeleton investigated.

Many points in the mass spectra of these alkaloids did not lend themselves to unambiguous interpretation without the aid of either: (a) extensive isotopic labeling; and/or (b) accurate mass measurement of high resolution mass spectra. For this reason, it seemed most expedient to record the high resolution fragmentation patterns of selected members of this class of alkaloid. It seemed particularly appropriate to initiate a detailed study of the mass spectral fragmentation in a series of alkaloids not having an aromatic moiety, which would not allow utilization of the mass spectrometric shift technique so fruitfully employed in structure work in the indole-dihydroindole series of alkaloids [6], and recently in the Amaryllidaceae alkaloids [5].

The Lycopodium alkaloids which have been the subject of our present high resolution studies are members of the skeletal type of lycopodine (4) and annotinine (8).

For the purposes of discussion of the fragmentation modes of the basal carbon skeleton represented by lycopodine (4) and the effect of functionality on such an alicyclic ring system, it is convenient to consider the members containing a C-4 hydrogen atom in one group and those with functional groups (no C-4 hydrogen atom) at C-4 separately. This distinction was made by MacLean [7] in discussion of the low resolution mass spectra, in which it was demonstrated that removal of the C-4 hydrogen, by functionality or double bond formation in the 3,4-position, prevents the facile loss
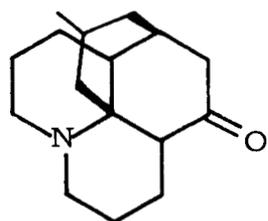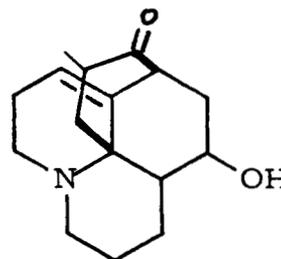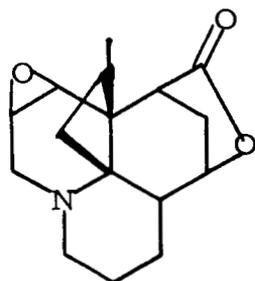
Lycopodine (4)
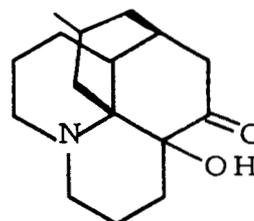
flabelliformine (5)
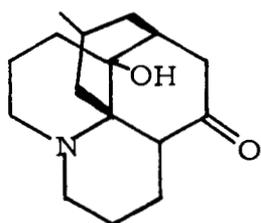
lycodoline (6)

Acrifoline (7)

Annotinine (8)

TABLE 2

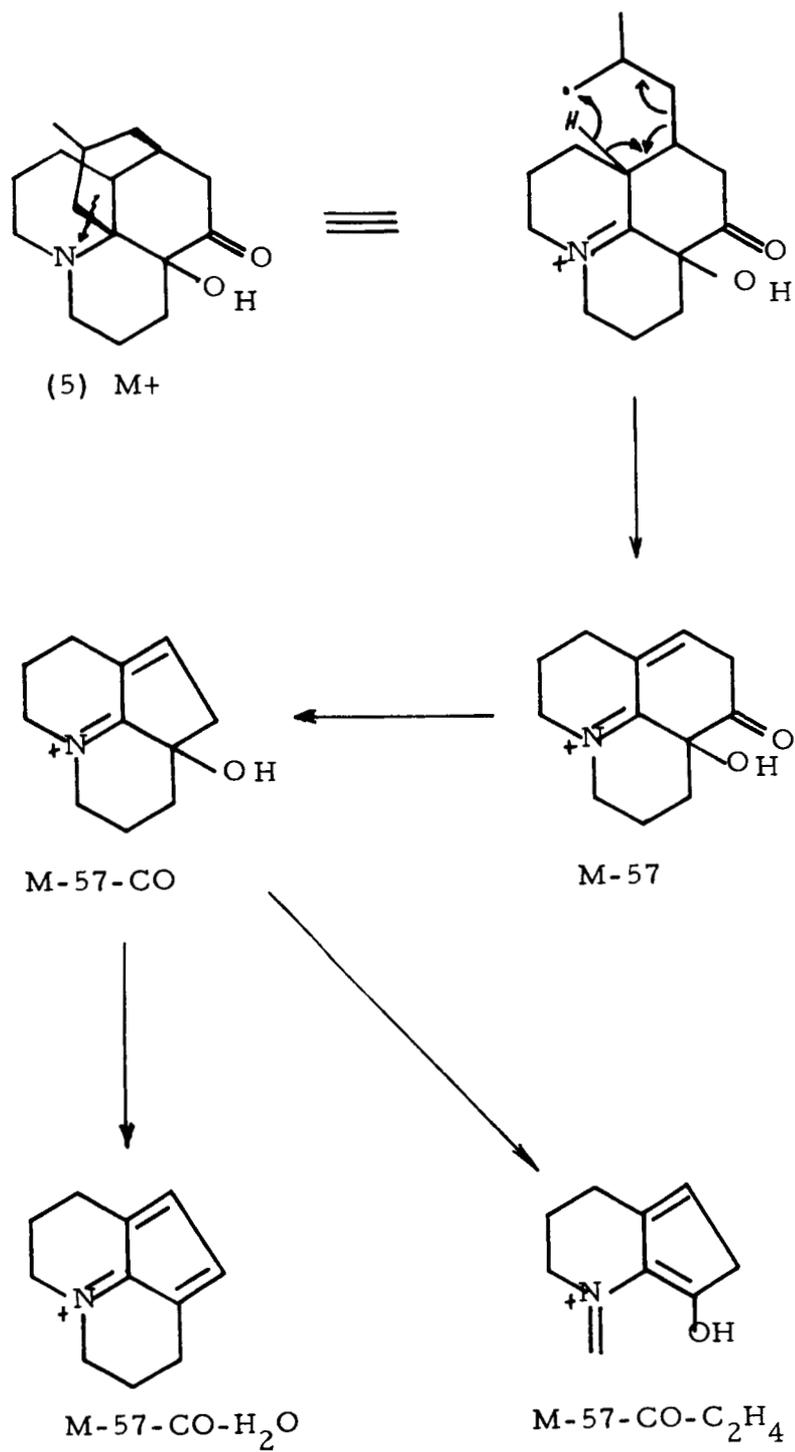Accurate mass measurement of Lycopodine (4) .

measured mass	error (obs. -calc.) in m. m. u.	elemental composition
134.0591	-1.5	C_8H_8NO
134.0975	+0.5	$C_9H_{12}N$
136.1128	+0.2	$C_9H_{14}N$
137.1195	-0.9	$C_9H_{15}N$
150.0905	-1.4	$C_9H_{12}NO$
150.1266	-1.7	$C_{10}H_{16}N$
160.1095	-3.1	$C_{11}H_{14}N$
162.0895	-2.5	$C_{10}H_{12}NO$
162.1270	-1.3	$C_{11}H_{16}N$
163.1342	-1.9	$C_{11}H_{17}N$
174.1255	-2.8	$C_{12}H_{16}N$
176.1039	-3.6	$C_{11}H_{14}NO$
176.1429	-1.0	$C_{12}H_{18}N$
190.1238	+0.6	$C_{12}H_{16}N$
204.1414	+2.6	$C_{13}H_{18}NO$
232.1645	-5.6	$C_{15}H_{22}NO$
244.1650	-5.1	$C_{16}H_{22}NO$
245.1741	-3.9	$C_{16}H_{23}NO$
247.1986	+5.0	$C_{16}H_{25}NO$
248.2020	-1.2	$C_{15}C^{13}H_{25}NO$

of the bridge (C-13, C-14, C-15, C-16) with concomitant migration of the

C-4 hydrogen resulting in the very large fragment at M-57 (C_4H_7) (see

Scheme IIa). The low resolution mass spectrum of lycopodine (4) is repro-

duced in Figure 4 and indicates clearly that the major mode of electron-impact-

induced decomposition in this alicyclic ring system proceeds with loss of the

four carbon bridge plus a hydrogen atom. Ions at M-43 and M-57 are con-

firmed to contain $C_{13}H_{18}NO$ and $C_{12}H_{16}NO$, respectively as indicated in

Table 2. Additional significant peaks in the spectrum of lycopodine occur

at M-85 and M-143 and appear due to sequential loss of 28 mass units twice

from the extremely intense ion at m/e 190. As indicated in Table 2, the

high resolution mass spectrogram shows M-85 to be an O-CH_4 doublet of

approximate equal intensity indicating that both the loss of carbon monoxide

and ethylene as neutral species are equally facile modes of decomposition

from the singlet peak at m/e 190. Further loss of 28 m.u. from m/e 162

results in the O-CH_4 doublet at m/e 134 (M-143) -- the major ion having

the composition, $C_9H_{12}N$. The minor component is probably formed from

two successive losses of ethylene from m/e 190, since it has the composition,

C_8H_8NO.

Flabelliformine (5):

The general features of the conventional mass spectrum (Figure 5)

of flabelliformine (8-hydroxylycopodine) are easily understood in terms of

the dominant mode of decomposition in lycopodine itself, with the exception

incurred where the 8-hydroxy group plays a significant role by facilitating

a pathway not energetically favorable in lycopodine. In Table 3 are listed

the accurate masses and empirical compositions of the major ions in the

high resolution mass spectrum of flabelliformine (5). Those peaks obviously

analogous to lycopodine are depicted in Scheme IIa and require no further

discussion, i.e. M-43, M-57, M-57-18, etc. However, it should be noted

SCHEME IIa

(5) M+

M-57-CO

M-57

M-57-CO-H$_2$O

M-57-CO-C$_2$H$_4$

'that a large peak has appeared at M-99 in this compound which has not been encountered in this carbon skeleton before [7]. High resolution reveals the M-99 peak to be a doublet of approximately equal ion current, and accurate mass measurement establishes the empirical compositions to be $C_{10}H_{14}NO$ and $C_{11}H_{18}N$ as shown in Table 3. From conventional mass spectrometric studies, MacLean [7] suggested two possible fragment ion structures containing one and two oxygen atoms for the M-99 peak which would account for the presence of this large ion only in this compound, i. e.:

M-57
($C_{12}H_{16}NO_2$)

M-99
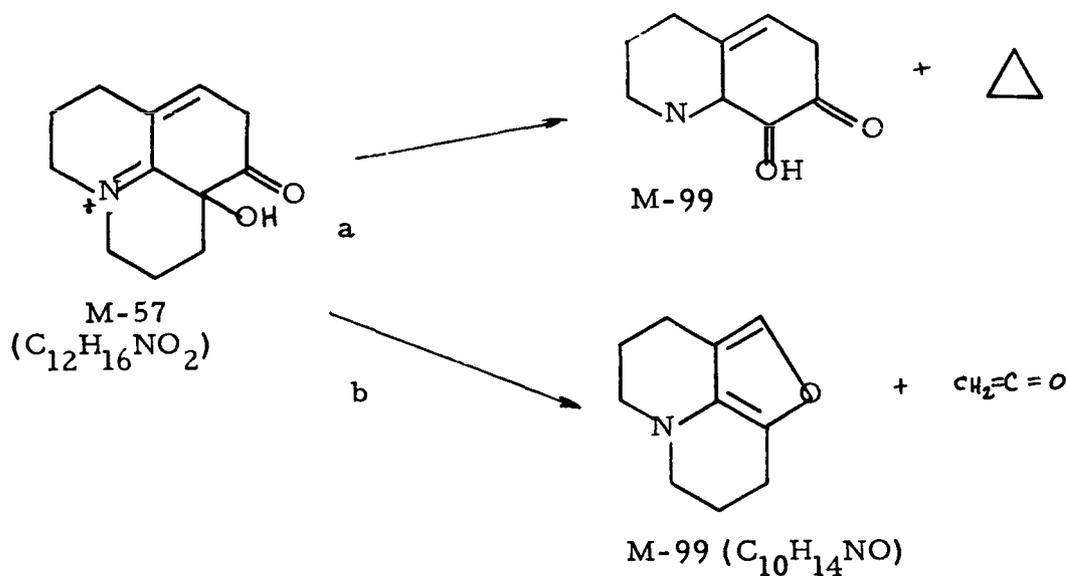
M-99 ($C_{10}H_{14}NO$)

It can be seen that fragment "b" above would account for the $C_{10}H_{14}NO$ fragment arising via loss of ketene from the M-57 peak. However, the empirical composition, $C_{11}H_{18}N$, rules out the possibility of its genesis in the M-57 ion (whose composition is $C_{12}H_{16}NO_2$). A more detailed analysis of the accurate mass data in Table 3 for flabelliformine reveals further that the $C_{12}H_{20}N$ species in the O-CH_4-doublet at m/e 178 cannot arise from the M-57 peak either -- although the oxygen containing component ($C_{11}H_{16}NO$) can be explained through loss of carbon monoxide as a neutral fragment from the M-57 peak. A fragmentation pathway is proposed in Scheme IIb for the formation of these two peaks from the molecular
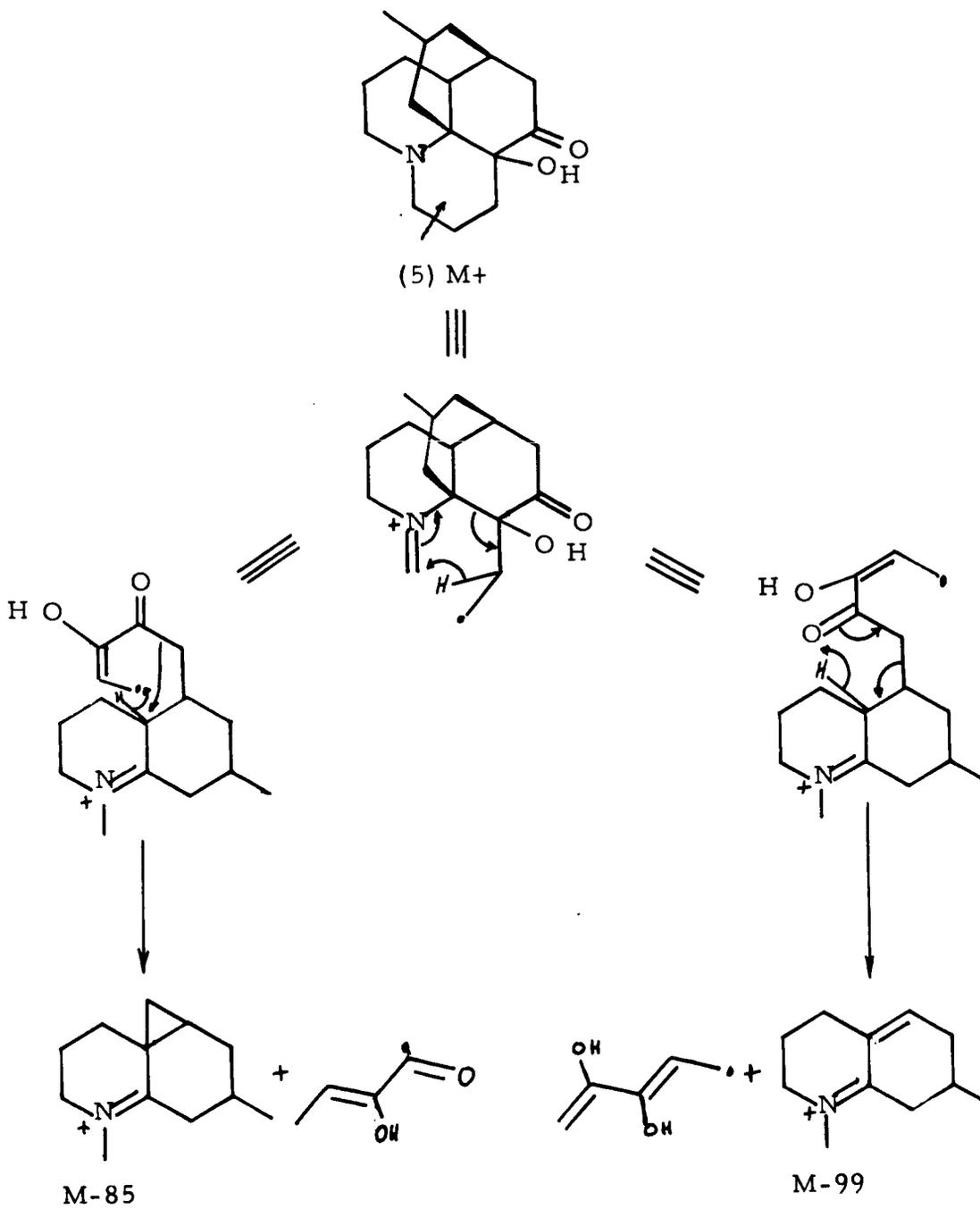
SCHEME IIb

(5) M+

M-85

M-99

TABLE 3

Accurate mass measurement of Flabelliformine (5).

Measured mass	error (obs. -calc.) in m. m. u.	elemental composition	measured mass	error (obs. -calc.) in m. m. u.	elemental composition
132.0803	-1.0	$C_9H_{10}N$	174.1273	-1.0	$C_{12}H_{16}N$
134.0958	-1.2	$C_9H_{12}N$	176.1082	+0.7	$C_{11}H_{14}NO$
136.0746	-1.6	$C_8H_{10}NO$	176.1409	-3.0	$C_{12}H_{18}N$
136.1122	-0.4	$C_9H_{14}N$	178.0762	-2.0	$C_{14}H_{10}$
138.0890	-2.9	$C_8H_{12}NO$	178.1218	-1.4	$C_{11}H_{16}NO$
138.1258	-2.5	$C_9H_{16}N$	178.1573	-2.3	$C_{12}H_{20}N$
146.0931	-3.9	$C_{10}H_{12}N$	206.1219	+3.8	$C_{12}H_{16}NO_2$
148.1109	-1.7	$C_{10}H_{14}N$	207.1280	+2.1	$C_{12}H_{17}NO_2$
150.0903	-1.6	$C_9H_{12}NO$	220.1340	+0.3	$C_{13}H_{18}NO_2$
150.1264	-1.9	$C_{10}H_{16}N$	221.1396	-2.0	$C_{13}H_{19}NO_2$
152.1053	-2.2	$C_9H_{14}NO$	245.1785	+0.5	$C_{16}H_{23}NO$
160.1088	-3.8	$C_{11}H_{14}N$	246.1897	+3.9	$C_{16}H_{24}NO$
164.1078	+0.3	$C_{10}H_{14}NO$	247.1910	-2.6	$C_{16}H_{25}NO$
164.1431	-0.8	$C_{11}H_{18}N$	248.1688	+3.8	$C_{15}H_{22}NO_2$
165.1131	-2.3	$C_{10}H_{15}NO$	262.1823	+1.6	$C_{16}H_{24}NO_2$
165.1509	-0.8	$C_{11}H_{19}N$	264.1966	+0.3	$C_{16}H_{26}NO_2$
172.1090	-3.6	$C_{12}H_{14}N$			

ion of flabelliformine (5). Labeling studies are in progress to ascertain the mechanism of the hydrogen transfer steps in the proposed scheme.

It can be seen from this illustration the advantage of having the empirical composition of all peaks in a high resolution mass spectrum available to descern more subtle features in the possible modes of molecular decomposition on electron impact, and clarify their dependence on small changes in molecular structure.

Since the conventional mass spectra of other representatives of this carbon skeleton having a hydrogen atom at C-4 are reported [7] as simple fragmentation patterns quite analogous to lycopodine, their spectra are easily interpreted in terms of the fragmentation mechanisms already presented. Our attention is now turned to representatives of the Lycopodium alkaloids having substituents at C-4.

Lycodoline (6) and Acrifoline (7):

From the low resolution mass spectrum (Figure 6) of lycodoline (6), it is immediately apparent that the lack of a hydrogen at C-4 severly hampers the previously facile elimination of the four carbon bridge, forcing the molecule to fragment in a much less specific manner -- the result being a large number of relatively intense fragments. This conclusion is further emphasized by the greatly attenuated contribution of the M-56 and M-57 peaks to the total ionization of the molecule. Accurate mass measurement confirms the nature of these two peaks as singlets having lost hydrocarbon moieties, see Table 4. An energetically comparable pathway now appears to proceed via loss of neutral ethylene from the M-43 peak giving rise to a singlet at m/e 192 (M-71, $C_3H_7 + C_2H_4$). A somewhat more favorable process is reflected in the loss of 73 m. u. (C_4H_9O) from the molecular ion, probably initiated by loss of a hydroxyl radical followed by the four carbon bridge, to form the peak at m/e 190. As in the case of lycopodine, this fragment

TABLE 4

Accurate mass measurement of Lycodoline (6)

measured mass	error (obs.-calc.) in m.m.u.	elemental composition	measured mass	error (obs.-calc.) in m.m.u.	elemental composition
122.0621	+1.5	C_7H_8NO	165.0685	-1.9	$C_{13}H_9$
122.0971	+0.1	$C_8H_{12}N$	165.1130	-2.4	$C_{10}H_{15}NO$
123.1058	+1.0	$C_8H_{13}N$	178.0840	-2.8	$C_{10}H_{12}NO_2$
124.0759	-0.3	$C_7H_{10}NO$	178.1225	-0.7	$C_{11}H_{16}NO$
124.1112	-1.4	$C_8H_{14}N$	188.0737	+2.6	$C_{11}H_{10}NO_2$
130.0622	-3.5	C_9H_8N	188.1436	-0.3	$C_{13}H_{18}N$
132.0787	-2.6	$C_9H_{10}N$	190.1256	+2.4	$C_{12}H_{16}NO$
134.0940	-3.0	$C_9H_{12}N$	192.1018	-0.6	$C_{11}H_{14}NO_2$
136.0753	-0.9	$C_8H_{10}NO$	206.1186	+0.5	$C_{12}H_{16}NO_2$
136.1111	-1.5	$C_9H_{14}N$	207.1266	+0.7	$C_{12}H_{17}NO_2$
150.0916	-0.3	$C_9H_{12}NO$	218.1903	-0.6	$C_{15}H_{24}N$
150.1270	-1.3	$C_{10}H_{16}N$	220.1354	+1.7	$C_{13}H_{18}NO_2$
151.0527	-2.1	$C_{12}H_{17}$	230.1517	-2.8	$C_{15}H_{20}NO$
151.0999	+0.2	$C_9H_{13}NO$	235.1938	+0.2	$C_{15}H_{25}NO$
152.0605	-2.1	$C_{12}H_8$	244.1685	-1.6	$C_{16}H_{22}NO$
152.1056	-1.9	$C_9H_{14}NO$	245.1771	-0.9	$C_{16}H_{23}NO$
160.0763	+0.1	$C_{10}H_{10}NO$	246.1864	+0.6	$C_{16}H_{24}NO$
160.1116	-1.0	$C_{11}H_{14}N$	248.1668	+1.8	$C_{15}H_{22}NO_2$
162.0904	-1.5	$C_{10}H_{12}NO$	263.1895	+1.0	$C_{16}H_{25}NO_2$
162.1260	-2.3	$C_{11}H_{16}N$			

can now lose either carbon monoxide or ethylene as neutral species -- processes documented by the accurate mass measurement of the $O-CH_4$- doublet at m/e 162 and the singlet at m/e 134 ($C_9H_{12}N$).

Peaks at M-17, M-17-28, and M-28 are due to appropriate losses of hydroxyl radical and neutral carbon monoxide from the molecular ion.

Turning now to the high resolution fragmentation pattern of acrifoline (7) which lacks a C-4 hydrogen by virtue of a double bond in the 3.,4-position, peaks at M-28, M-70 and M-87 are the most intense. Although detailed analysis of the high resolution data on all major fragments confirms the various modes of decomposition available to the basal carbon skeleton, several points should be mentioned. The M-28 peak appears as a doublet for the first time in these spectra, both *via* elimination of CO and C_2H_4 from the molecular ion. The M-43 peak proved to be composed of an $O-CH_4$-doublet of approximately equal intensity, thus offering some indication that the $M-C_3H_7$ which have occurred in all of these spectra are from the bridge carbons. A minor doublet occurs at m/e 216 arising by loss of a hydroxyl radical from the doublet at M-28.

Mechanisms proposed by MacLean for the formation of the peaks at M-70 and M-87 are consistant with the accurate mass data presented in Table 5 for acrifoline (7).

In conclusion, it should be stated that, even though the placement of substituents in positions which severely retard particularily facile modes of fragmentation in this alicyclic alkaloidal structure, and change the general appearance of conventional mass spectra to a drastic extent in some cases, careful analysis of all peaks in a high resolution mass spect- rogram offers the unique advantage of using all of the information contained in the peaks of lesser abundance. The result is to make use of this myriad of data to confirm and establish confidence in assignment of fragmentation mechanisms and fragment structures, rather than relying on only the

TABLE 5

Accurate mass measurement of Acrifoline (7)

measured mass	error (obs.-calc.) in m.m.m.	elemental composition	measured mass	error (obs.-calc.) in m.m.u.	elemental composition
117.0612	+3.4	C_8H_7N	190.1226	-0.6	$C_{12}H_{16}NO$
118.0658	+0.1	C_8H_8N	191.1325	+1.5	$C_{12}H_{17}NO$
119.0717	-1.8	C_8H_9N	192.1343	-4.5	$C_{12}H_{18}NO$
120.0811	-0.2	$C_8H_{10}N$	204.1390	+0.2	$C_{13}H_{18}NO$
123.1042	-0.6	$C_8H_{13}N$	216.1003	-2.1	$C_{13}H_{14}NO_2$
130.0678	+2.1	C_9H_8N	216.1392	+0.4	$C_{14}H_{18}NO$
132.0824	+1.1	$C_9H_{10}N$	216.1740	-1.2	$C_{15}H_{22}N$
134.0963	-0.7	$C_9H_{12}N$	217.1429	-3.7	$C_{14}H_{19}NO$
144.0821	+0.8	$C_{10}H_{10}N$	218.1181	0.0	$C_{13}H_{16}NO_2$
146.0620	+1.4	C_9H_8NO	218.1540	-0.5	$C_{14}H_{20}NO$
146.0992	+2.2	$C_{10}H_{12}N$	232.1330	-0.7	$C_{14}H_{18}NO_2$
147.1054	+0.6	$C_{10}H_{13}N$	232.1700	-0.1	$C_{15}H_{22}NO$
160.0777	+1.5	$C_{10}H_{10}NO$	233.1410	-0.6	$C_{14}H_{19}NO_2$
160.1130	+0.4	$C_{11}H_{14}N$	233.1785	+0.5	$C_{15}H_{23}NO$
162.0921	+0.2	$C_{10}H_{12}NO$	242.1530	-1.5	$C_{16}H_{20}NO$
162.1276	-0.7	$C_{11}H_{16}N$	243.1606	-1.7	$C_{16}H_{21}NO$
170.0961	-0.9	$C_{12}H_{12}N$	244.1679	-2.2	$C_{16}H_{22}NO$
172.1116	-1.0	$C_{12}H_{14}N$	245.1728	-5.2	$C_{16}H_{23}NO$
174.1302	+1.9	$C_{12}H_{16}N$	246.1493	-0.1	$C_{15}H_{20}NO_2$
175.1355	-0.6	$C_{12}H_{17}N$	260.1665	+1.5	$C_{16}H_{22}NO_2$
176.1067	-0.8	$C_{11}H_{14}NO$	261.1785	+5.6	$C_{16}H_{23}NO_2$

energetically most favorable processes resulting in the few very abundant ions in a low resolution mass spectrum.

Annotinine (8):

The feature which distinguishes annotinine (8) from other Lycopodium alkaloids in this study is the three carbon bridge forming a four membered ring at C-4, C-12. From the nominal mass spectrum (Figure 7) it can be seen that facile loss of the bridge as propylene is indicated by the large M-42 peak compared with the molecular ion. Large peaks at M-71, M-86, and M-115 form the remaining large fragments as seen in Figure 7.

As will become apparent from analysis of the accurate mass measurement of annotinine, which are listed in Table 5, the M-42 peak is important, not only in that it enables a distinction to be made which characterizes this carbon skeleton in contrast to the lycopodine (4) type, but it directs the remaining modes of cleavage in the molecule. The fragmentation sequences are proposed in Scheme III. Major peaks at m/e 204 and 189 arise via loss of carbon monoxide and carbon dioxide, respectively, from the peak at M-42.

It is interesting to note that the composition of the relatively small peak at m/e 190 is partly due to the ^{13}C isotope of m/e 189 ($C_{12}H_{15}NO$), and partly to an ion whose composition is $C_{11}H_{12}NO_2$. Retro-Diels-Alder cleavage of ring B in the M-42 fragment (See Scheme III) with subsequent cleavage of the ester bond yields the dienone of composition $C_{11}H_{12}NO_2$.

SCHEME III

(8) M+
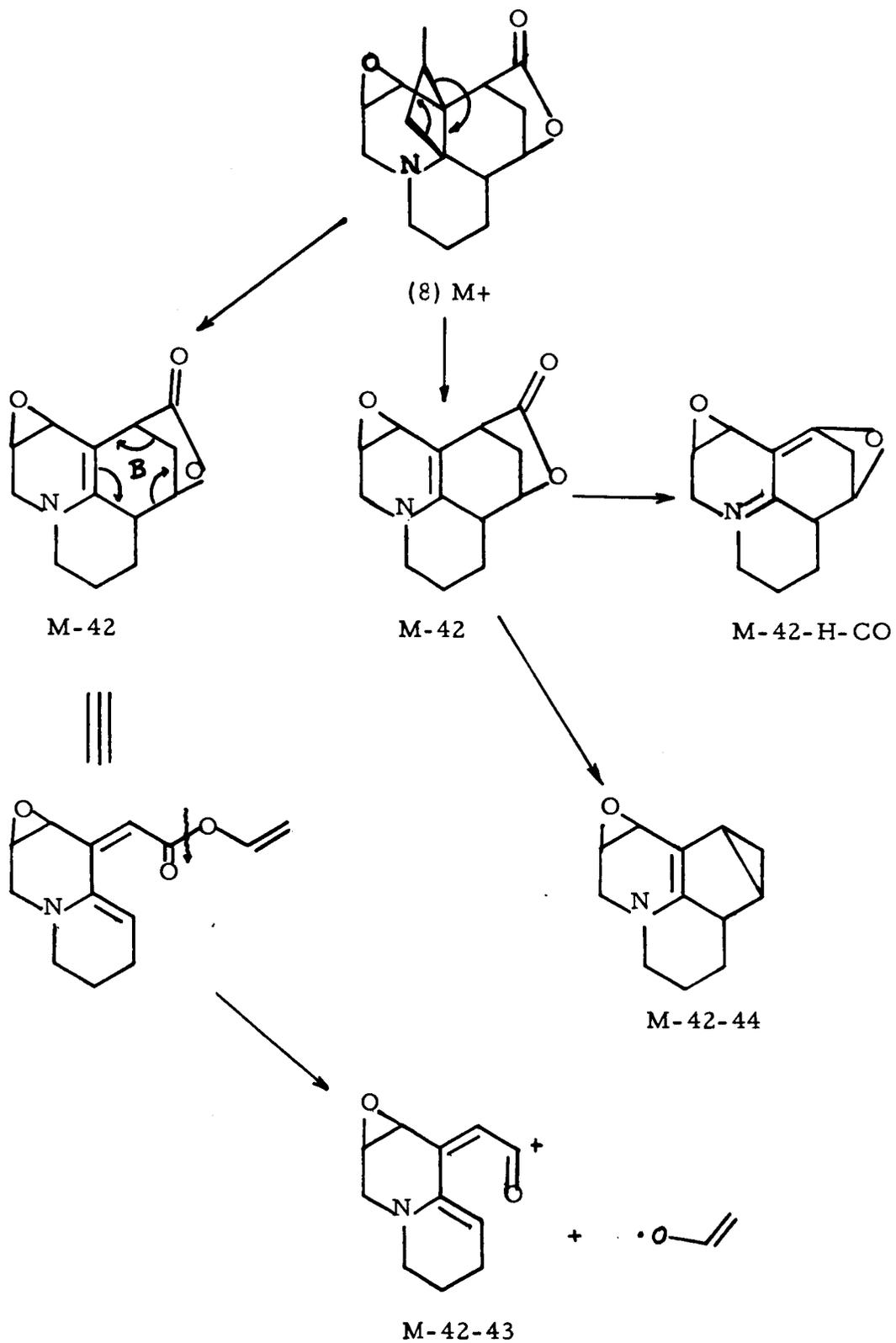
M-42

M-42

M-42-H-CO

M-42-44

M-42-43

TABLE 6

Accurate mass measurement of Annotinine (8)

measured mass	error (obs.-calc.) in m.m.u.	elemental composition	measured mass	error (obs.-calc.) in m.m.u.	elemental composition
120.0439	-1.0	C_7H_6NO	170.0998	+2.8	$C_{12}H_{12}N$
120.0829	+1.5	$C_8H_{10}N$	172.0775	+1.3	$C_{11}H_{10}NO$
121.0888	-0.4	$C_8H_{11}N$	172.1142	+1.6	$C_{12}H_{14}N$
122.0978	+0.8	$C_8H_{12}N$	174.0920	+0.1	$C_{11}H_{12}NO$
130.0657	0.0	C_9H_8N	174.1289	+0.6	$C_{12}H_{16}N$
132.0562	-1.3	C_9H_8O	176.1093	+1.8	$C_{11}H_{14}NO$
132.0827	+1.4	$C_9H_{10}N$	177.1165	+0.9	$C_{11}H_{15}NO$
133.0614	-3.9	C_9H_9O	188.1077	+0.2	$C_{12}H_{14}NO$
133.0902	+1.1	$C_9H_{11}N$	189.1173	+1.9	$C_{12}H_{15}NO$
134.0960	-1.0	$C_9H_{12}N$	190.0859	-0.9	$C_{11}H_{12}NO$
144.0812	-0.1	$C_{10}H_{10}N$	190.1191	-4.1	$C_{12}H_{16}NO$
146.0614	+0.8	C_9H_8NO	204.1055	+3.1	$C_{12}H_{14}NO_2$
146.0974	+0.4	$C_{10}H_{12}N$	205.1076	-2.7	$C_{12}H_{15}NO_2$
148.0761	-0.1	$C_9H_{10}NO$	214.0870	+0.2	$C_{13}H_{12}NO_2$
148.1148	+2.2	$C_{10}H_{14}N$	216.1016	-0.8	$C_{13}H_{14}NO_2$
158.0954	+1.1	$C_8H_{14}O_3$	232.0974	0.0	$C_{13}H_{14}NO_3$
160.0772	+1.0	$C_{10}H_{10}NO$	233.1071	+1.9	$C_{13}H_{15}NO_3$
160.1173	+4.7	$C_{11}H_{14}N$	234.1116	-1.4	$C_{13}H_{16}NO_3$
161.0843	+0.2	$C_{10}H_{11}NO$	246.1451	-4.3	$C_{15}H_{20}NO_2$
161.1209	+0.5	$C_{11}H_{15}N$	257.1422	+0.6	$C_{16}H_{19}NO_2$
			275.1551	+3.0	$C_{16}H_{21}NO_3$

Conclusions:

The automatic data reduction of high-resolution mass spectrograms has provided accurate measurements with average deviations in the order of 1.5 millimass units under normal operating conditions.

The empirical compositions of the fragments represented by lines in high resolution mass spectra have provided a detailed knowledge of the fragmentation pathways in the two skeletal systems reported.

The vast quantity of precise information derivable from such an approach to high resolution mass spectrometry cannot be over emphasized.

It is apparent that high resolution mass spectrometry can play a unique role in the unambiguous structural characterization of minute amounts of organic materials encountered in chemical and biological research.

Bibliography:

1. J. H. Beynon, "Mass Spectrometry and its Application to Organic Chemistry", Elsevier Publishing Company, 1960.

2. K. Biemann, Eleventh Annual Conference on Mass Spectrometry and Related Topics, ASTM Committee E-14, May 19-24, 1963, San Francisco, California, pp. 235-240.

3. K. Biemann, P. Bommer, A. L. Burlingame, and W. J. McMurray, Tetrahedron Letters No. 28, pp. 1969-1973 (1963).

4. P. Bommer, W. J. McMurray and K. Biemann, J. Am. Chem. Soc., 86, 1439 (1964).

5. A. L. Burlingame, H. Fales and R. J. Highet, J. Am. Chem. Soc. submitted.

6. K. Biemann, Mass Spectrometry, McGraw Hill Book Company, 1962, ch. 8.

7. D. B. MacLean, Can. J. Chem., 41, 2654 (1963).

FIGURE 1, DIRECT SAMPLE INLET SYSTEM

A.   To Isatron

B.   Tungsten Heater Wire

C.   Inside Surface Silvered

D.   All Glass Valve

E.   To Diffusion Pump

F.   Gold Leak

G.   Inlet System

H.   Kovar Seal

I.   4 mm Constriction

J.   In Line Valve

K.   Teflon Sample Holder and Seal

L.   Stop

M.   To Diffusion Pump

N.   To Rough Pump

O.   Quick Disconnect Nut

P.   Teflon Chevron Seal

Q.   Sample Handle

FIG. 2.   BUPHANISINE

FIG. 3.   DIHYDROBUPHANISINE

FIG. 4.   LYCOPODINE

FIG. 5.   FLABELLIFORMINE

FIG. 6. LYCODOLINE

FIG. 7. ANNOTININE